AFRL-AFOSR-UK-TR-2014-0050

New physical constraints for multi-frame blind deconvolution

Dr. Szymon Gładysz (Principal Investigator) with:
Dr. Roberto Baena Gallé (Royal Academy of Sciences and Arts of Barcelona and University of Barcelona, Spain)
Dr. Venkata Gudimetla (Air Force Research Laboratory)
Dr. Julian Christou (Large Binocular Telescope Observatory)

REAL ACADEMIA DE CIENCIAS Y ARTES DE BARCELONA
RAMBLA DE LOS ESTUDIOS 115
BARCELONA, 08002 SPAIN

EOARD Grant 12-2115

Report Date: December 2014

Final Report from 1 September 2012 to 31 August 2014

Air Force Research Laboratory
Air Force Office of Scientific Research
European Office of Aerospace Research and Development
Unit 4515, APO AE 09421-4515

REPORT DOCUMENTATION PAGE

Form Approved OMB No. 0704-0188

1. REPORT DATE *(DD-MM-YYYY)*	2. REPORT TYPE	3. DATES COVERED *(From – To)*
10 December 2014	Final Report	1 September 2012 – 31 August 2014

4. TITLE AND SUBTITLE

New physical constraints for multi-frame blind deconvolution

5a. CONTRACT NUMBER

FA8655-12-1-2115

5b. GRANT NUMBER

Grant 12-2115

5c. PROGRAM ELEMENT NUMBER

61102F

6. AUTHOR(S)

Dr. Szymon Gładysz (Principal Investigator) with:
Dr. Roberto Baena Gallé (Royal Academy of Sciences and Arts of Barcelona and University of Barcelona, Spain)
Dr. Venkata Gudimetla (Air Force Research Laboratory)
Dr. Julian Christou (Large Binocular Telescope Observatory)

5d. PROJECT NUMBER

5d. TASK NUMBER

5e. WORK UNIT NUMBER

7. PERFORMING ORGANIZATION NAME(S) AND ADDRESS(ES)

REAL ACADEMIA DE CIENCIAS Y ARTES DE BARCELONA
RAMBLA DE LOS ESTUDIOS 115
BARCELONA, 08002 SPAIN

8. PERFORMING ORGANIZATION REPORT NUMBER

N/A

9. SPONSORING/MONITORING AGENCY NAME(S) AND ADDRESS(ES)

EOARD
Unit 4515
APO AE 09421-4515

10. SPONSOR/MONITOR'S ACRONYM(S)

AFRL/AFOSR/IOE (EOARD)

11. SPONSOR/MONITOR'S REPORT NUMBER(S)

AFRL-AFOSR-UK-TR-2014-0050

12. DISTRIBUTION/AVAILABILITY STATEMENT

Distribution A: Approved for public release; distribution is unlimited.

13. SUPPLEMENTARY NOTES

14. ABSTRACT

This work extended on previous efforts to explore state-of the-art blind image deconvolution techniques for improving space surveillance capabilities. The project had two objectives: (1) to develop and test a new theory of speckle statistics based on the model of partially-developed speckle, and (2) to test if inclusion of this theory in deconvolution removes the need for human intervention. Using a physics-based approach to exploit knowledge of the whole imaging process, the goal is to have a fully automatic process that could eventually approach real-time capabilities. The first year resulted in an Adaptive Wavelets Maximum Likelihood Estimator (AWMLE) algorithm for adaptive optics assisted observations (public release) while the second year focused on modelling of spatial, temporal and spectral integration of speckle statistics. Including constraints in Fourier domain, this work led to a novel methodology of testing the reconstruction fidelity in the image reconstruction process. Overall, this project has developed new models for statistics of speckle images based on a theory which is fundamentally different from the approaches developed in the 1970s. When checked against baseline theory, this new multi-frame blind deconvolution approach proved extraordinarily good performance while exhibiting autonomous capabilities.

15. SUBJECT TERMS

EOARD, adaptive optics, image post-processing, speckle statistics, deconvolution, space surveillance, optronics

16. SECURITY CLASSIFICATION OF:			17. LIMITATION OF ABSTRACT	18, NUMBER OF PAGES	19a. NAME OF RESPONSIBLE PERSON
a. REPORT	b. ABSTRACT	c. THIS PAGE			Kevin Bollino
UNCLAS	UNCLAS	UNCLAS	SAR	14	19b. TELEPHONE NUMBER *(Include area code)* +44 (0)1895 616163

Dr. Szymon Gładysz 10 December 2014

Fraunhofer Institute of Optronics,
System Technologies and Image Exploitation IOSB
Gutleuthausstraße 1, 76275 Ettlingen, Germany
Phone +49 7243 992 120
szymon.gladysz@iosb.fraunhofer.de

Grant number FA8655-12-1-2115

"New physical constraints for multi-frame blind deconvolution"

Final report

Period of performance: 9.1.2013 - 8.31.2014

Szymon Gładysz (Principal Investigator) with:

Roberto Baena Gallé (Royal Academy of Sciences and Arts of Barcelona and University of Barcelona, Spain)

Venkata Gudimetla (Air Force Research Laboratory)

Julian Christou (Large Binocular Telescope Observatory)

Table of Contents

List of Figures

1. Summary

In this document we report on activities related to the project “New physical constraints for multi-frame blind deconvolution”, grant number FA8655-12-1-2115, in the second year of funding. Based on theoretical work on speckle statistics in the first year of the project we developed a deconvolution algorithm which outperforms state of the art, while being free of parameters which normally have to be tweaked by the user.

In what follows, we summarize all relevant developments, also some from Year 1, and give examples of results obtained on the AFRL’s 3.5m SOR telescope in New Mexico.

2. Introduction

Images of space objects taken with ground-based telescopes are blurred by atmospheric turbulence. The problem can be alleviated by the use of adaptive optics (AO) and/or image post-processing. Adaptive optics systems work well in infrared but they struggle at shorter wavelengths. With AO in the visible, attainment of diffraction-limited resolution is currently only possible in conjunction with subsequent deconvolution (Figure 1). An optimal way to process AO images is the one based on the knowledge of the whole imaging process: starting from the influence of turbulence, through the optical system and its aberrations, and ending with (partial) image correction by AO. Such a physics-based approach, if it could be made fully automatic, would reduce the need for human intervention.

Currently, the most popular approach to deconvolution of AO images is the so-called “blind” deconvolution which relinquishes the afore-mentioned determinism. Instead, it is assumed that smart computer algorithms will find the optimal way to deconvolve the data. On the other hand blind deconvolution is rarely executed blindly. All available methods have parameters which the user fine-tunes until the most visually-appealing reconstruction is achieved. The “art” of deconvolution is to find constraints which allow for the best estimate of an object to be recovered, but in practice these parameterized constraints often reduce deconvolution to the struggle of trial and error.

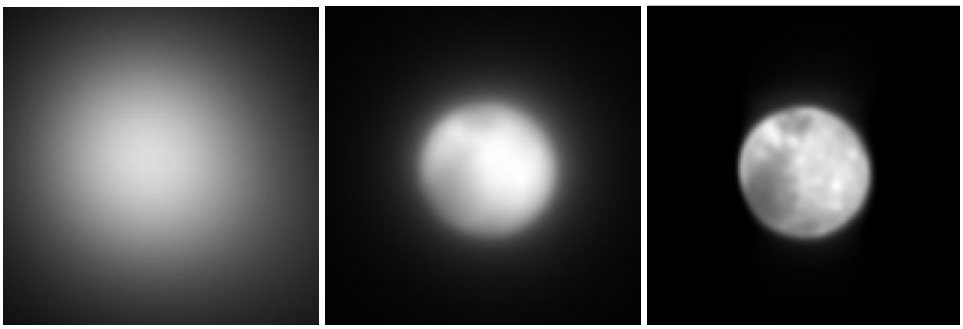

Fig. 1. Images of Jupiter’s moon Ganymede. Left: summation of thousand short exposures, no AO. Middle: AO switched on. Right: AO data after blind deconvolution. For deconvolution we used MISTRAL package [1]. Data taken with the AFRL’s 3.5m telescope in New Mexico at Starfire Optical Range (SOR), wavelength of the observations was 850nm, AO system is based on a Shack-Hartmann sensor with 24 × 24 subapertures.

The project had two objectives: (1) to develop and test a new theory of speckle statistics based on the model of partially-developed speckle, and (2) to test if inclusion of this theory in deconvolution removes the need for human intervention.

3. Methods, Assumptions, and Procedures

In the first year of the project we performed a large set of experiments involving four state-of-the-art deconvolution algorithms. The setup of the experiments and conclusions were reported in the interim report and also published in a journal paper [2] therefore we will not expand on them here. Worth mentioning is that the Adaptive Wavelets Maximum Likelihood Estimator (AWMLE) algorithm developed as part of the project for AO-assisted observations was subsequently re-written, documented and packaged for public release in 2014.

In the second year of funding, analytical work on modelling of spatial, temporal and spectral integration of speckle statistics was carried out. Constraints in Fourier domain were also worked out. A novel methodology of testing the reconstruction fidelity was put forward. These aspects of our work are detailed in the following sections.

3.1 Integrated speckle statistics

It is well known that integration (e.g. adding of several independent realizations in one pixel) changes speckle statistics [3]. This is an important problem in imaging through turbulence because one of the most widely spread solution to the problem, speckle imaging, relies on non-integrated speckle in order to work. On the other hand, very little in the way of analytical modelling of the effect of integration (for example, increasing the exposure time of the observations) has been attempted. To our knowledge, only one author attacked this problem but the resulting formulas are rather complex and have dependencies on several parameters which cannot be obtained from the data, like phase variance [4]. We aimed to provide an alternative, simple description of the effect of integration on various speckle statistics.

Figure 2 illustrates the problem. The integration parameter, *M*, is small in the top row and large in the bottom row. *M* can be thought of as a number of speckles contributing to one pixel. While the change in *M* due to spatial and temporal integration has been the subject of some attention in the context of scattering of rough surfaces [3], the spectral component of *M* has not, and this constitutes our contribution. Imagining a discrete set of increasing wavelengths, producing radially expanding PSFs, we see that stepping over wavelengths results in new speckles traversing a pixel under observation if it is away from the PSF center. The further a pixel is from the center the more speckles will traverse it (compare the sharp speckles close in to the smooth streaks further out from the center in the rightmost column of Figure 2).

We proposed analytical solutions based on the definition of *M* (ratio of spatial, temporal or spectral auto-correlations of speckle and pixel shape) and empirical solutions based on relation of *M* to first-order speckle statistics:

$$M = \frac{\langle \mathbf{h}(x,y) \rangle^2}{\mathrm{var}(\mathbf{h}(x,y))} = \mu\nu\tau \tag{1}$$

where $\mathbf{h}(x, y)$ is one speckle pattern, $\langle . \rangle$ stands for mean value and var(.) stands for variance. The symbols μ, ν and τ are spatial, spectral and temporal integration parameters. The first two need only be estimated once for a given detector and filter. This is the approach we took for the results presented here. The third parameter was estimated by computing the ratio of M in simulated, noise-free, instantaneous-exposure-time simulations to M from real observations at SOR. This way, it was found to be around 5 for our datasets [5]. An illustration of proper choice of τ is shown in Figure 3, where this parameter was varied around 5 to test the effect on reconstruction of one particular speckle frame from SOR observations. This can be considered an independent test for our estimation strategy for τ. The methodology pertaining to checking the fidelity of reconstructions is elucidated in Section 3.3.

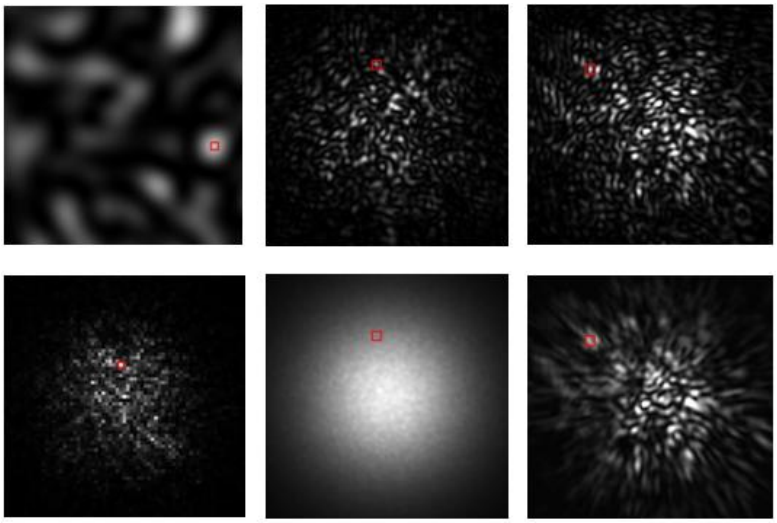

Fig. 2. Visual effect of integration: spatial (left column), temporal (middle column) and spectral (rightmost column). For each case a red square was used to denote the extent of one pixel. All images are simulated. In the top row pixels are physically small, exposure time of the simulated observations is very short (or rather instantaneous) and the band-pass of the simulated filter is negligible (monochromatic observations). In the bottom row the situation was reversed: the pixel size is large compared to speckle dimension, as many as 10 000 short exposures were summed, and filter band-pass is 100 nm (which can be considered large for speckle imaging).

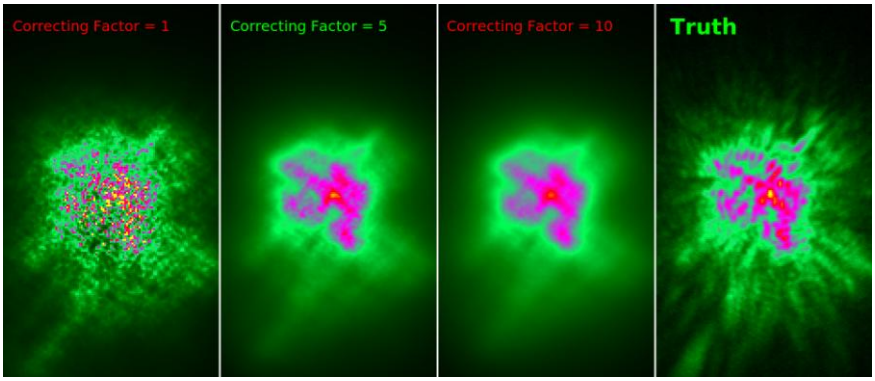

Fig. 3. Reconstructions of one particular speckle frame (PSF) based on various choices for the temporal integration parameter (spatial and spectral integration parameters had been calculated beforehand and fixed). The rightmost panel shows the ground-truth image. Artificial color coding and square-root scale.

3.2 Fourier-domain constraint

In our work we rely on rigorous Bayesian formulation of the problem of finding a true object **o** and a (stochastic) PSF **h** which together with noise generated the recorded data **i**:

$$p(\mathbf{o},\mathbf{h}\mid\mathbf{i}) = \frac{p(\mathbf{i}\mid\mathbf{o},\mathbf{h})\cdot p(\mathbf{o})\cdot p(\mathbf{h})}{p(\mathbf{i})} \tag{2}$$

The theorem states that the conditional probability of the object being equal to reconstruction **o** and the PSF being equal to reconstruction **h** given that we recorded data **i**, is equal to the product of: conditional probability of the data taking on the value(s) **i** given **o** and **h**, probability of the object being equal to **o**, and the probability of the PSF being equal to **h**, divided by the probability of obtaining the data **i** which is always taken to be unity. In the maximum *a posteriori* (MAP) framework one finds estimates for the object, $\hat{\mathbf{o}}$, and the PSF(s), $\hat{\mathbf{h}}$, which jointly maximize $p(\mathbf{o},\mathbf{h}|\mathbf{i})$:

$$[\hat{\mathbf{o}},\hat{\mathbf{h}}] = \arg\max_{\mathbf{o},\,\mathbf{h}} p(\mathbf{o},\mathbf{h}|\mathbf{i}) = \arg\max_{\mathbf{o},\,\mathbf{h}} p(\mathbf{i}|\mathbf{o},\mathbf{h})\times p(\mathbf{o})\times p(\mathbf{h}) \tag{3}$$

Since a probability density function $p(\mathbf{o})$ for the object is in general not known, solutions in the form of functions with desirable mathematical properties (e.g. noise suppression, edge enhancement) are often used. As these *ad hoc* formulas are not real probability density functions (PDFs), regularization parameters must be used to balance their influence on the cost function in Equation (3). These parameters have to be chosen manually [1]. Apart from the problem of choosing the right value for them, the mere form of the prior (e.g. an object's power spectral density) could be applicable only to a limited class of real objects. For these reasons we focus on PSF statistics $p(\mathbf{h})$. This part of Equation (3) was almost always removed from the MAP approach but we have shown how useful it is.

In Year 1 of the project we focused on the gamma distribution for the focal-plane intensity statistics of **h**. For this purpose we developed the general framework for inclusion of the integration parameter for intensity (Section 3.1). We also proved that the gamma PDF provides a good model for the integrated speckle (spatially, temporally and spectrally) [6]. In Year 2 we also developed a constraint in the Fourier domain (where Fourier domain means Fourier transformed focal-plane intensity). Under the assumption of normal distribution of the real and imaginary parts of the optical transfer function (OTF), one has a complete model for their joint statistics:

$$\begin{aligned}
\langle \Re \rangle &= e^{-\frac{D_\phi(\mathbf{u})}{2}}, \\
\langle \Im \rangle &= 0, \\
\mathrm{var}(\Re) &= \frac{1}{2m(\mathbf{u})}\left[1 + e^{-2D_\phi(\mathbf{u})} - 2e^{-D_\phi(\mathbf{u})}\right], \\
\mathrm{var}(\Im) &= \frac{1}{2m(\mathbf{u})}\left[1 - e^{-2D_\phi(\mathbf{u})}\right]
\end{aligned} \tag{4}$$

where $D_\phi(\mathbf{u})$ is the phase structure function evaluated for 2-D spatial frequency **u** and $m(\mathbf{u})$ is the number of OTF "cells" at that frequency (both allowing for non-isotropic turbulence) [7].

This prior was implemented in multi-frame blind deconvolution algorithm. Its performance is illustrated on simulated observations in Figure 4 (real I-band speckle PSFs from SOR were convolved with a schematic representation of the Hubble Space Telescope which acted as the true object).

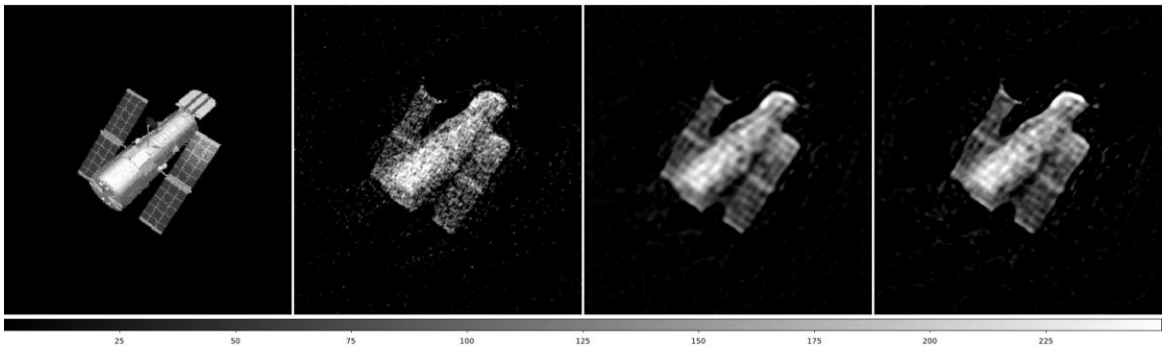

Fig. 4. True object (leftmost panel) and three reconstructions (from left to right: without any prior, with the spatial constraint gamma prior, and with the Fourier constraint prior). Refer to Figure 5 for illustration of the blurred input data.

3.3 Testing reconstruction fidelity

Figures 4 and 5 are typical of what is shown in most image processing papers. Reconstructions of the objects are successful even for significant blur and noise corruption (Figure 5, bottom row). On the other hand we are putting constraints on the PSFs, not on the objects, and therefore it is more interesting to check the accuracy of the PSF reconstructions. In our tests we fixed the object and we tasked the algorithm with reconstructing the PSFs only. This way we could check the benefit of applying our analytical models for the PSF prior.

We allowed the algorithm to perform 20 000 iterations. The convergence of reconstructed patterns to ground-truth speckle frames was clearly visible beyond ca. 4000 iterations. This is shown in Figure 6. More extensive testing and the corresponding results are discussed in Section 4.

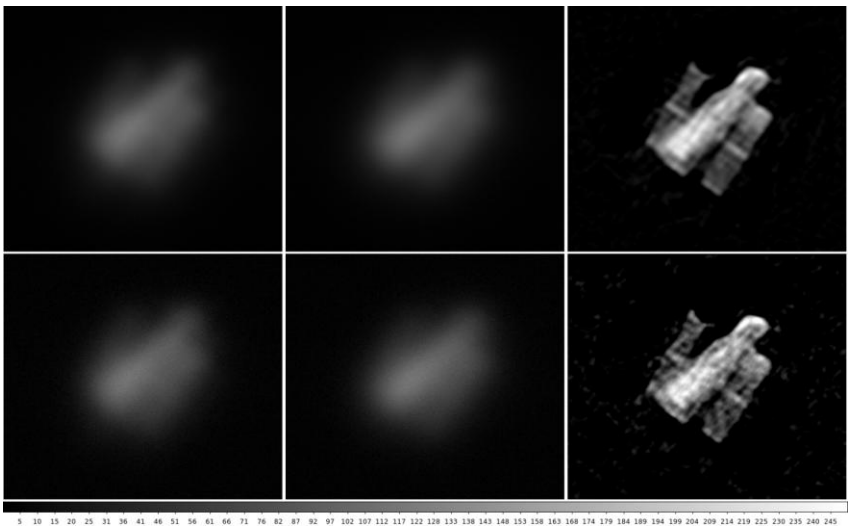

Fig. 5. From left to right: one input data frame, long exposure, and reconstructions obtained with our MFBD code. Top row: signal-to-noise ratio (SNR) of the simulated observations was 100. Bottom row: SNR was 20.

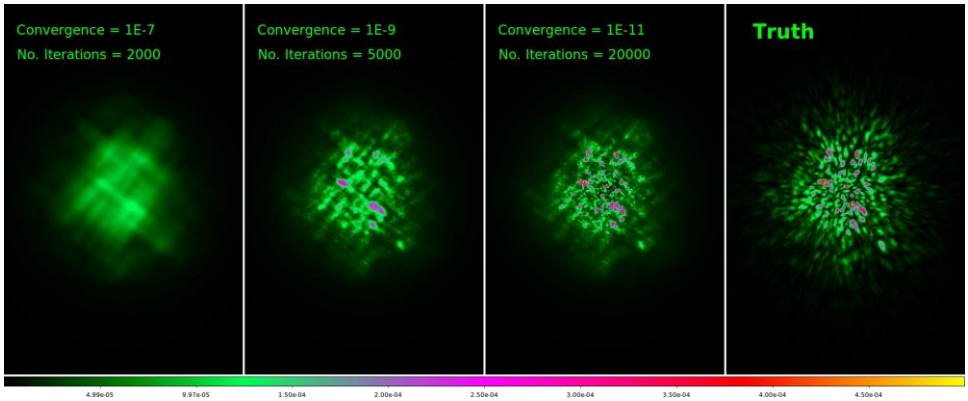

Fig. 6. Illustration of the algorithm's convergence. The code was supplied with perfectly known, fixed object and only PSFs were reconstructed.

4. Results and Discussion

In Year 2 our main mode of checking algorithm's performance was by looking at how well it reconstructed the ground-truth PSFs. We were interested in how the algorithm performs, given: low-SNR conditions, bad initial guess for the average PSF, or integration parameter *M* in the gamma model for the intensity prior.

In general, it was observed that the new priors significantly helped in delaying the onset of noise amplification. They basically provided for the same regularization mechanism as traditional object priors, with the major difference that PSF priors are based on physical models of the aberrating medium (turbulence) and not on properties of the objects being imaged (which are by definition unknown). This is the main contribution of our work.

Figure 7 shows how a lack of prior in traditional, maximum-likelihood deconvolution leads to very noisy reconstructions. This is avoided by applying a gamma prior on PSF intensity (central panel).

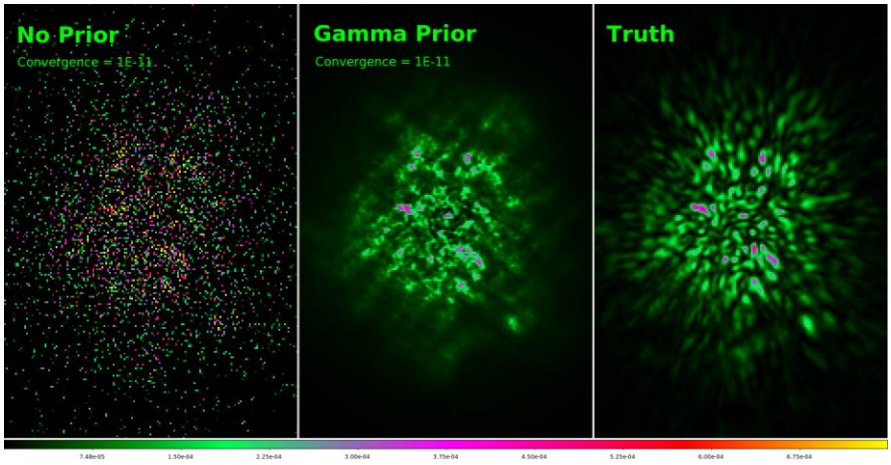

Fig. 7. PSF-prior based reconstruction vs. a no-prior execution. In both cases the algorithm was supplied with a true object and allowed to iterate on the PSFs (20 000 iterations).

Another important aspect of our work, pursued in Year 1, was estimation of average PSF directly from the target observations. This, in principle, allows one to save observing time (because point-source calibrators are not needed) and algorithm execution time (because the trial-and-error guessing of the correct first-guess PSF is eliminated). In order to remove the object being viewed from the image formation equation an object cancelling transformation was proposed [8]. After transforming the data, information about the object cancels out, and one is left only with moments of the turbulent OTF which is customary parameterized by the Fried parameter r_0. In our tests this method achieves accuracy of around 10% on r_0 for realistic simulations with Gaussian noise, broadband filter ($\Delta\lambda/\lambda = 0.2$) and only 100 input frames (Figure 8).

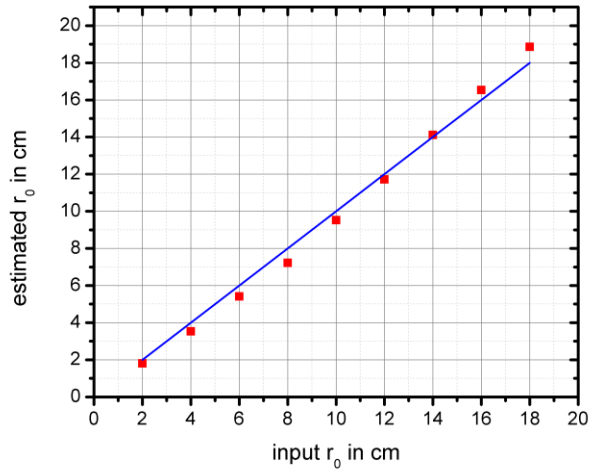

Fig. 8. Demonstration of the accuracy of the "Fourier contrast" r_0 estimation method. Based on simulated observations of artificial satellites with a 0.5 m telescope.

In Year 2 we checked how important this first guess for the average PSF is for successful reconstructions of the individual speckle PSFs. We supplied the algorithm with r_0 from the "Fourier contrast" method [8,9] which was almost equal to the ground-truth r_0, and also with a deliberately mismatched r_0. The results show that the effect of wrong first guess becomes especially visible at low SNR, as expected.

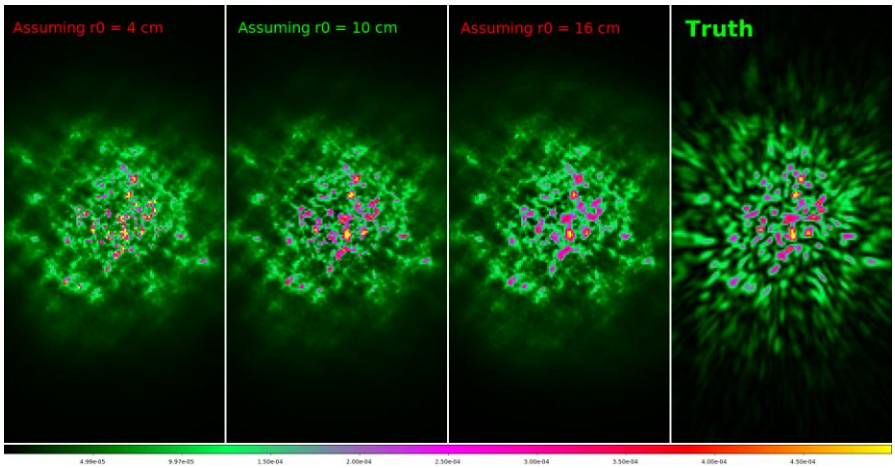

Fig. 9. Assuming wrong r_0 has little impact on PSF reconstruction quality when SNR of the dataset is high (here 100). The true r_0 was 10 cm.

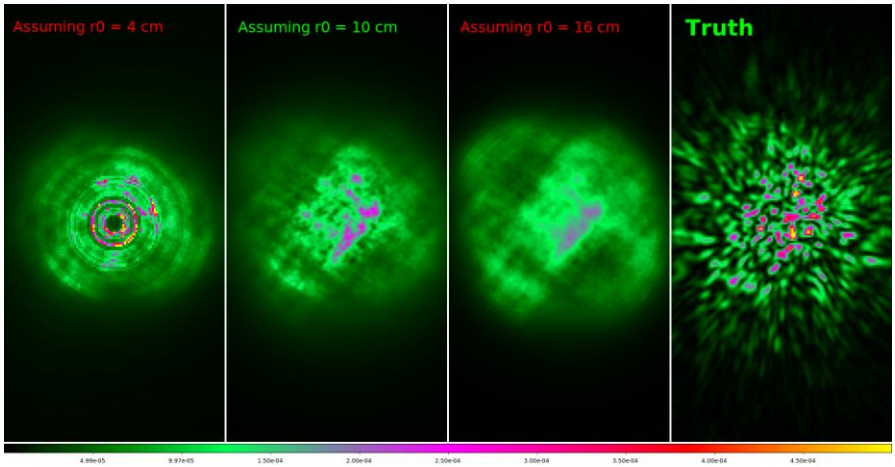

Fig. 10. Incorrect first guess for r_0 (and correspondingly for the average PSF) leads to badly reconstructed PSFs when SNR is low (here 20). This is especially visible for underestimated r_0 (leftmost panel).

5. Conclusions

In our project "New physical constraints for multi-frame blind deconvolution", grant number FA8655-12-1-2115, we have developed new models for statistics of speckle images. The models are based on a theory which is fundamentally different from the approaches developed in the 1970s for speckle imaging. We make use of the equations developed for scattering off rough surfaces ("partially-developed speckle"). The models were checked against the baseline theory.

This theory was employed in the task of restoring the quality of images taken through turbulence. In blind tests, the new multi-frame blind deconvolution provided significantly better image quality than one of the codes used by AFRL personnel at SOR. Our MFBD code can be executed autonomously, i.e. without tweaking of parameters and without specifying a first-guess PSF. The project has resulted so far in one journal paper (two more in preparation) and five papers in conference proceedings.

6. References

1. Laurent M. Mugnier, Thierry Fusco, and Jean-Marc Conan, "MISTRAL: a myopic edge-preserving image restoration method, with application to astronomical adaptive-optics-corrected long-exposure images," J. Opt. Soc. Am. A 21, 1841-1854 (2004).

2. Roberto Baena Galle, Jorge Nunez, Szymon Gladysz, "Extended-object reconstruction in adaptive-optics imaging: the multiresolution approach", Astronomy & Astrophysics, 555, A69, (2013).

3. Joseph W. Goodman, Speckle Phenomena in Optics (Roberts & Company Publishers, 2006)

4. Junji Ohtsubo, "Effects of finite spectral bandwidth and focusing error on the transfer function in stellar speckle interferometry," J. Opt. Soc. Am. A 2, 667-673 (1985).

5. Roberto Baena Galle, Szymon Gladysz, Laurent Mugnier, Rao Gudimetla, Robert Johnson, and Lee Kann, "Blind Deconvolution of Turbulence-degraded Images Using Natural PSF Priors," in Imaging and Applied Optics 2014, The Optical Society, (2014).

6. Roberto Baena Galle, Szymon Gladysz, Laurent Mugnier, Venkata Gudimetla, Robert Johnson, and Lee Kann, "Unsupervised blind deconvolution," Proceedings of the AMOS Technical Conference, 9-13 September 2013, Maui, Hawaii, (2013).

7. Roberto Baena Galle, Szymon Gladysz, Laurent Mugnier, Rao Gudimetla, Robert Johnson, and Lee Kann, "Physically-constrained Multi-frame Blind Deconvolution," in Imaging and Applied Optics, J. Christou and D. Miller, eds., OSA Technical Digest (online) (Optical Society of America, 2013), paper JW2A.3, (2013).

8. Szymon Gladysz, Roberto Baena Gallé, Robert Johnson, and Lee Kann, "Image reconstruction of extended objects: demonstration with the Starfire Optical Range 3.5m telescope," Proceedings of SPIE, Volume 8535, 85350M-1-13 (2012).

9. Szymon Gladysz, "Estimation of turbulence strength directly from target images," in Imaging and Applied Optics, J. Christou and D. Miller, eds., OSA Technical Digest (online) (Optical Society of America, 2013), paper JW1A.4, 2013.

7. List of Symbols, Abbreviations, and Acronyms

AO – adaptive optics

AWMLE – adaptive wavelets maximum-likelihood estimator

MFBD – multi-frame blind deconvolution

PDF – probability density function

PSF – point-spread function

SNR – signal-to-noise ratio